*Bull. Mater. Sci.* (2020) 43:132
https://doi.org/10.1007/s12034-020-02134-2





# Shear thickening fluid based on silica with neodymium oxide nanoparticles

**LI SUN[1], YINRU LV[1], MINGHAI WEI[2,*], HONG SUN[1] and JIE ZHU[1]**
[1]School of Civil Engineering, Shenyang Jianzhu University, Shenyang 110168, China
[2]Department of Construction and Engineering Management, Shenyang Jianzhu Univeristy, Shenyang 110168, China
*Author for correspondence (wei.mgh@gmail.com)

MS received 27 October 2019; accepted 4 May 2020; published online 4 June 2020

**Abstract.** The rheological performance of shear thickening fluid (STF) based on silica with neodymium oxide nanoparticles ($Nd_2O_3/SiO_2$-STF) was investigated in this study. $Nd_2O_3/SiO_2$-STF suspensions of varied concentrations (9–15 wt%) were prepared using an ultrasonic oscillator. The presence of $Nd_2O_3$ particle and its interaction with silica nanoparticles in the $Nd_2O_3/SiO_2$-STF were analysed using scanning electron microscopy, X-ray diffractometry and energy dispersive spectroscopy. $Nd_2O_3/SiO_2$ interaction demonstrated that silica nanoparticle could be completely attached on the needle branches of the $Nd_2O_3$ particles, and formed a considerable clustering effect. The steady rheological testing results indicated that an appropriate amount of $Nd_2O_3$ particle resulted in a marked increase in the peak viscosity from 51.95 ($SiO_2$-STF) to 218.94 Pa.s ($Nd_2O_3/SiO_2$-STF), and a concomitant decrease in the critical shear rate from 199.65 ($SiO_2$-STF) to 50.18 $s^{-1}$ ($Nd_2O_3/SiO_2$-STF). Moreover, although the peak viscosity declined with the rise in temperature, shear thickening was remarkable compared to those of $SiO_2$-STF and became highly remarkable with $Nd_2O_3$ particle mass fraction increase.

**Keywords.** Shear thickening fluid; neodymium oxide; silica; shear thickening effect; temperature.

## 1. Introduction

Shear thickening fluid (STF) is a kind of high concentration colloidal suspension, which is composed of monodisperse nanoparticles suspended in a carrier fluid [1–4]. It has the ability to transform from fluidity to rigidity when suddenly stimulated. During this transversion, STF absorbs a lot of impact energy and induce significant damping effect. Therefore, STFs can be used as a base material for fibres or fabrics to improve its impact properties [5–8]. They are also used as a single damping material in vibration control devices to obtain excellent energy dissipation capacity [9–11]. However, the shear thickening (ST) behaviour and environmental temperature significantly impact the mechanical performance of the fabrics/fibres and devices. Therefore, studies related to advanced STFs with specific requirements of higher viscosity and highly obvious ST effects at high temperature are essential.

Ge *et al* [12] investigated the rheological performance of the STF strengthened with the silicon carbide nanowires (SiC-STF). As per the results, the initial and the ST viscosity of SiC-STF demonstrated an increase of approximately 30% compared to those of the signal STF. Gürgen *et al* [13] added the SiC nanoparticles to silicon-based STF ($SiO_2$-STF) to investigate its rheological properties, and indicated that the SiC nanoparticle addition can significantly increase the initial viscosity of $SiO_2$-STF, reduce its thickening rate, and delay its activation by controlling the thickening time. Sha *et al* [14] employed carbon fibres, graphene and silicon dioxide as dispersing phases and polyethylene glycol (PEG) as the dispersing media to prepare a series of STFs in combination with different dispersing phases. It was discovered that the addition of carbon nanotubes can improve the ST performance, while graphene demonstrates the opposite effect. However, carbon nanotubes and graphene can be added in appropriate proportions to achieve different functions of the STF. The effect of CNFs on the rheological characteristics of $SiO_2$-STF was investigated by Ghosh *et al* [15]. The results showed that the intersection of energy dissipation and storage modulus occurred at higher angular frequencies, when the content of the CNFs increased, indicating that the addition of the CNFs enhanced the ST effect of $SiO_2$-STF.

With respect to the dispersed media, Jiang *et al* [16] studied the rheological behaviour of polymethylmethacrylate particle suspensions in glycerine–water (3:1) mixtures and established that these suspensions demonstrate not only excellent reversible and thixotropic properties, but also a strong ST behaviour. STFs with varied molecular chain lengths of PEG were investigated by Xu *et al* [17]. The results indicated that the ST effect significantly improved with an increase in the molecular chain length. Qin *et al* [18] investigated the viscoelasticity of STF with different mass fraction silica nanoparticle in ionic liquid and 1-butyl-3-methylimidizolium tetrafluoroborate. Experimental results established that all the dispersions demonstrated shear thinning, notable ST and shear thinning successively with increase in shear rate. For

the common $SiO_2$-STF, Tian *et al* [19] also showed that high temperatures had significant influence on the critical shear rate and ST effect. The above researches confirmed that the STFs had different rheological characteristics with different dispersed particles and media. However, there have only been limited investigations in the literature about the effect of neodymium oxide ($Nd_2O_3$) additives on the rheological behaviour of the STFs.

To obtain the higher viscosity and highly obvious ST effects at high temperature, tombarthite neodymium is used as addition in this study. Neodymium particles have attracted immense interest in composite materials science [20–22] due to their excellent small-size effect, interfacial surface effect, quantum size effect and tunnelling effect. In this study, first, $Nd_2O_3$ particles were characterized and dispersed into PEG200 to prepare a $Nd_2O_3/SiO_2$-STF suspension. Then, the rheological behaviour of the $Nd_2O_3/SiO_2$-STF suspension with different $Nd_2O_3/SiO_2$ mass ratio values was evaluated using steady shear testing. Finally, the effect of temperature on $Nd_2O_3/SiO_2$-STF suspension's ST performance was discussed.

## 2. Experimental

### 2.1 *Materials*

In this study, the silica nanoparticles (AEROSIL200) are hydrophilic, gas-phase silica with a primary particle size of 12 nm. The hydroxyl value of PEG200 is 510−623 mg KOH $g^{-1}$, which is a stable transparent liquid at room temperature. The neodymium nanoparticles are a light blue solid powder with a density of 7.24 g $ml^{-1}$ and a molecular weight of 336.47, and an average diameter of 5 μm. The N-[3-(trimethoxysilyl) propyl] ethyl are used as dispersant. Its boiling point, molecular weight, and density of diamine are 261°C, 222.36 and 1.03 g $ml^{-1}$, respectively.

### 2.2 *Preparation of STF*

The silica and neodymium nanoparticles are first dried in a vacuum drying chamber for 12 h before the preparation of $Nd_2O_3/SiO_2$-STFs. In the preparation process, the water bath is maintained at a constant temperature, and appropriate amounts of PEG200 and the dispersant are stirred mechanically inside a beaker. Silica and neodymium nanoparticles are gradually added during stirring according to the mixing ratio of each suspension, and vibrated continuously with an ultrasonic oscillator until all the particles are evenly dispersed in PEG200 before the addition of $Nd_2O_3/SiO_2$-STFs. A stable $Nd_2O_3/SiO_2$-STF was obtained by placing it in a vacuum drying chamber at 110°C.

### 2.3 *Characterization and rheological performance test*

First, we took appropriate amounts of $Nd_2O_3$, silica and $Nd_2O_3/SiO_2$ (12:20) samples into absolute ethanol, and uniformly dispersed these samples by ultrasonic vibration. Then, after drying, a scanning electron microscope (SEM, S-4800, 40 kV) and an X-ray diffractometer (XRD) were used to analyse the morphological characteristics and the particles phase of these samples, respectively. The experimental conditions included radiation from a copper target. The voltage and current were, respectively, 40 kV and 30 mA, and its scanning speed was 8 degrees $min^{-1}$ under the range 5°−90° with 0.04° step length.

For the rheological properties investigated, the AR2000 rheometer was used to test the steady-state response of $Nd_2O_3/SiO_2$-STF with different mass ratio values. The diameter and spacing of the rheometer were 25 and 0.25 mm, respectively. The steady rheological tests were completed at temperatures 6.25, 12.25, 25 and 50°C, respectively.

## 3. Results and discussion

### 3.1 *Physical characterization*

Figure 1a–c shows the SEM images of the silica, $Nd_2O_3$ and $Nd_2O_3/SiO_2$ samples, respectively. It can be clearly observed from figure 1a that silica nanoparticle is a spherical particle of small size, and the agglomeration is severe. The SEM image in figure 1b shows that $Nd_2O_3$ is long and belongs to the micron level. One end of this nanoparticle demonstrates a tapered column shape, while the other has significantly irregular multi-needle branches. It is significantly different from

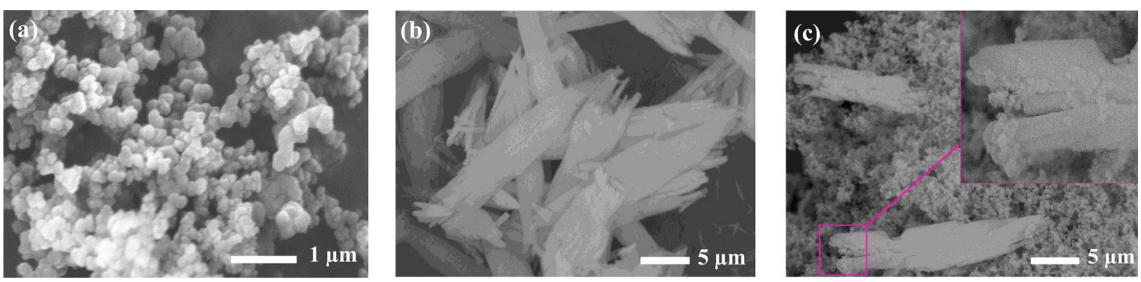


**Figure 1.** SEM micrographs of (**a**) silica; (**b**) $Nd_2O_3$ and (**c**) $Nd_2O_3/SiO_2$ samples.

the existing dispersed phase [15,23–25]. Figure 1c shows the SEM image of $Nd_2O_3/SiO_2$ combined at a mass ratio of 12:20. The following can be observed from the figure: the shapes of these two nanoparticles are completely different, the particle size of $Nd_2O_3$ is much larger than that of silica nanoparticle, and silica can be completely attached on the gap and needle branches of the $Nd_2O_3$ particles.

Figure 2 shows the results of the phase analysis performed using the XRD on the silica, $Nd_2O_3$ and the $Nd_2O_3/SiO_2$ samples. As observed in figure 2, silica nanoparticles demonstrate only one characteristic diffraction peak, which appeared in the range of $15°-25°$ . Then, the diffraction intensity of silica nanoparticles declined rapidly and tended to be stable with the diffraction angle increasing, indicating that silica nanoparticles are an amorphous material. As the half-peak width is inversely proportional to the particle size, a larger half-peak width also indicate that the silica particle size is smaller, which is nanoscale. In contrast, the diffraction peak of $Nd_2O_3$ particles is sharp and definite, and their positions are identical to that of the standard neodymium card (JPCDS card 01-074-2139), which establishes that the $Nd_2O_3$ sample is a single cubic crystal. The XRD diagram of the $Nd_2O_3/SiO_2$ samples is in the middle of the two peaks, which indicates that the system contains the silica and $Nd_2O_3$ samples.

To verify the constitution of the $Nd_2O_3/SiO_2$ sample, the energy dispersive spectroscopic (EDS) mapping was analysed. Figure 3a and b shows the scanning results of the O, Si and Nd elements after considering a specific EDS scanning area of the $Nd_2O_3/SiO_2$ sample. It can be seen from the figure that the distribution of all elements on the surface were significantly nonuniform, and even some concentration behaviour (bright spots) of the three elements can be observed. The mass fractions (wt%) of the above elements are 215.58 for O, 91.31 for Si and 8.11 for Nd, which indicate both silicon and neodymium exist in the sample.

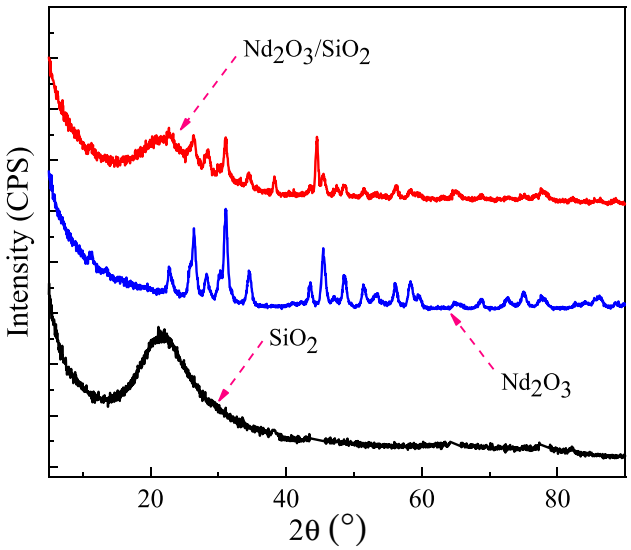


**Figure 2.** XRD patterns of different samples.

### 3.2 *Steady shear rheological properties of $Nd_2O_3/SiO_2$-STF*

Figure 4 shows the steady rheological properties of $Nd_2O_3/SiO_2$-STF with different mass ratio values within the shear rate scope of 0.1–1000 $s^{-1}$ at 25°C. Table 1 summarizes the characteristics of the four STF samples used in this study. Referring to figure 4a, compared to the $SiO_2$-STF, when the $Nd_2O_3$ particle mass fraction is 9%, the ST peak viscosity of $Nd_2O_3/SiO_2$-STF increased significantly from 51.95 to 145.91 Pa.s, while the critical shear rate decreased by 4 times to 10.00 $s^{-1}$. This indicates that the addition of $Nd_2O_3$ particle significantly improves the ST effect of $SiO_2$-STF. In contrast, the initial viscosity of $Nd_2O_3/SiO_2$-STF increased significantly by approximately 184 times from 1.87 to 345.97 Pa.s due to the addition of $Nd_2O_3$ particle, indicating that $Nd_2O_3/SiO_2$-STF demonstrates highly remarkable shear thinning characteristics. The reasons are as follows: first, $Nd_2O_3$ particle is a micron-sized particle of a large size,

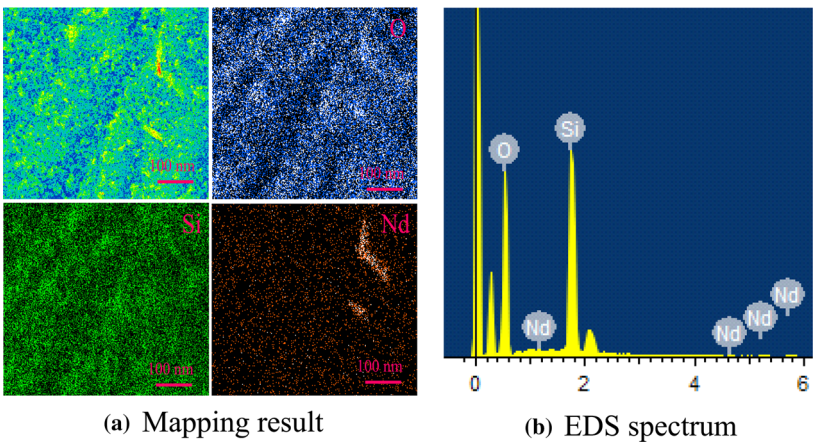


**Figure 3.** EDS spectrum scanning of $Nd_2O_3/SiO_2$ sample.

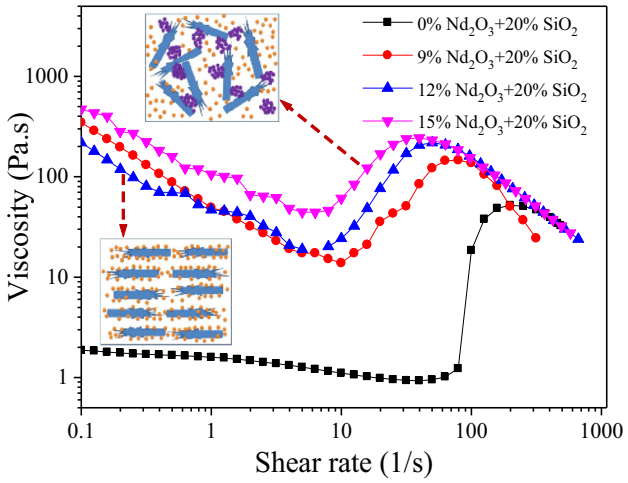


**Figure 4.** Steady shear rheological response of the $Nd_2O_3/SiO_2$-STF suspension.

which requires a large shear rate to drive the particle; second, when a small amount of $Nd_2O_3$ particle was added to $SiO_2$-STF, the particle content in the unit volume increased, distance between the particles decreased, and the opportunities of contact between the particles increased, resulting in the formation of agglomerations, which increases the flow friction force of the STF and significantly increases the initial viscosity.

As the mass fraction of $Nd_2O_3$ particle increased to 12%, compared to 9%$Nd_2O_3$/20%$SiO_2$-STF, although the critical shear rate of 12%$Nd_2O_3$/20%$SiO_2$-STF decreased slightly to 7.94 $s^{-1}$, the peak viscosity increased significantly by 50% from 145.91 to 218.94 Pa.s. Importantly, the initial viscosity decreased from 345.97 to 219.29 Pa.s, indicating that 12%$Nd_2O_3$/20%$SiO_2$-STF possesses good fluidity. This could be because, the nanosized silica was filled in the multiple needle branches at the end of $Nd_2O_3$ particle to form a superior gradation with $Nd_2O_3$ in the system, and $Nd_2O_3$ particle and silica nanoparticle were dispersed sufficiently in the whole system. In addition, the peak viscosity improved significantly due to the large particle size and high mass fraction of the agglomerated system.

When the mass fraction of $Nd_2O_3$ particle was increased to 15%, the critical shear rate of the suspension hardly decreased (still 7.94 $s^{-1}$), and its peak viscosity increased slightly from 218.94 to 244.03 Pa.s. Moreover, the initial viscosity of 15%$Nd_2O_3$/20%$SiO_2$-STF increased sharply to 470.52 Pa.s, indicating that the initial fluidity of the system had declined. One cause may be that a substantial amount of $Nd_2O_3$ particle from the suspension filled in the agglomeration gap, a larger shear rate was required to force it to flow, and the ST peak viscosity could not produce a higher clustering effect due to the heterogeneity of the particle size distribution in the system to form a higher peak viscosity.

### 3.3 *Temperature sensitivity of the $Nd_2O_3/SiO_2$ nanoparticle-based STF*

Figure 5a demonstrates the relationship between the complex viscosity and the oscillation strain of $SiO_2$-STF. It can be observed from the figure that with increase in temperature, both the initial and peak complex viscosity of $SiO_2$-STF decreased, while the critical shear rate increased slightly. This phenomenon is consistent with other literature experiments [19,26]. Importantly, when the temperature reached 50°C, the ST effect (STE) of $SiO_2$-STF decreased significantly. The peak viscosity was 29.02 Pa.s and the STE was 2.6, respectively. Therefore, it is evident that $SiO_2$-STF is not suitable for high temperature operation.

Figure 5b–d shows the relationship between the complex viscosity and oscillation strain of the $Nd_2O_3/SiO_2$-STF, with $Nd_2O_3$ particle mass fraction values of 9, 12 and 15% at different temperatures, respectively. It is observed from figure 5b–d that the critical shear rate and initial complex viscosity of $Nd_2O_3/SiO_2$-STF increased with increasing temperature. The higher the temperature, more significant the increase. For example, when the temperature increased from 25 to 50°C, the critical shear rate of the suspension not only increased by approximately 3.11 times from 79.26 to 326.11 $s^{-1}$, but also the initial complex viscosity increased significantly by approximately 14.68 times from 34.71 to 544.278 Pa.s.

## 4. Possible rheological mechanism for $Nd_2O_3/SiO_2$-STF

The remarkable shear thinning and ST behaviour of $Nd_2O_3/SiO_2$-STF is sketched in figure 6 and interpreted as follows. When a shear force acts on the $Nd_2O_3/SiO_2$-STF system,

**Table 1.** Summary of different $Nd_2O_3/SiO_2$-STF.

| $Nd_2O_3/SiO_2$-STF suspension | Initial point | Critical ST point | Peak point | Peak viscosity increase (Pa.s) |
|---|---|---|---|---|
| 0% $Nd_2O_3$ + 20% $SiO_2$ | 0.10 $s^{-1}$, 1.87 Pa.s | 50.0 $s^{-1}$, 0.95 Pa.s | 199.65 $s^{-1}$, 51.95 Pa.s | 51.00 |
| 9% $Nd_2O_3$ + 20% $SiO_2$ | 0.10 $s^{-1}$, 345.97 Pa.s | 10.00 $s^{-1}$, 13.85 Pa.s | 79.50 $s^{-1}$, 145.91 Pa.s | 132.06 |
| 12% $Nd_2O_3$ + 20% $SiO_2$ | 0.10 $s^{-1}$, 219.29 Pa.s | 7.94 $s^{-1}$, 20.13 Pa.s | 50.18 $s^{-1}$, 218.94 Pa.s | 198.81 |
| 15% $Nd_2O_3$ + 20% $SiO_2$ | 0.10 $s^{-1}$, 470.52 Pa.s | 7.94 $s^{-1}$, 46.21 Pa.s | 39.86 $s^{-1}$, 244.03 Pa.s | 197.82 |

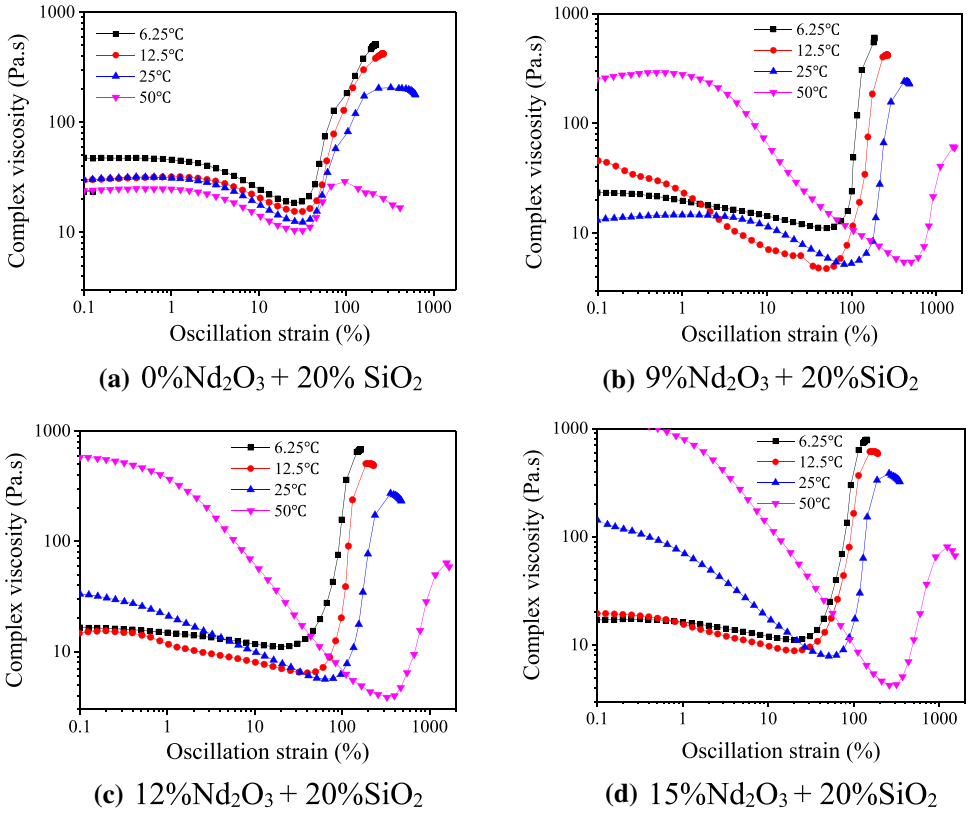


**Figure 5.** Complex viscosity *vs.* oscillation strain for $Nd_2O_3/SiO_2$-STF in various temperatures.

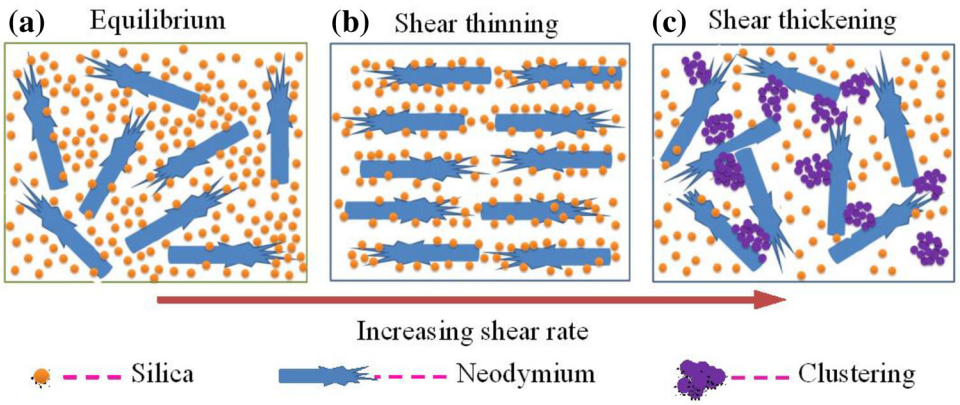


**Figure 6.** Schematic illustrations of physical reactions of $Nd_2O_3/SiO_2$-STF.

the system will be dominated by movements of the $Nd_2O_3$ particles and meanwhile, the $SiO_2$ particles adhere to the $Nd_2O_3$ particles. It is because the $Nd_2O_3$ particles are more and larger than the $SiO_2$ particles. As increasing the shear force and hence enhancing the shear rate, the $Nd_2O_3$ particles are changed from a chaotic state to a well-organized state and distributed uniformly as shown in figure 6b. As a consequence, the $Nd_2O_3/SiO_2$-STF exhibits an obvious shear thinning behaviour. However, when the shear rate increases to a threshold, the layered structure of $Nd_2O_3$ particle is destroyed, and the $Nd_2O_3$ particles are chaotic again, which obstructs fluid flow. Meanwhile, the $SiO_2$ particles adhering to the $Nd_2O_3$ particles also produces 'particle clusters' due to contact and extrusion, and further hinders fluid flow. Consequently, the viscosities of $Nd_2O_3/SiO_2$-STF increase. With further increasing the shear rate, more $Nd_2O_3$ particles are in a disordered state, and more $SiO_2$ particles form 'particle clusters'. The $Nd_2O_3$ particles produce 'particle clusters' through $SiO_2$ particles and hence form larger 'particle clusters' among $Nd_2O_3$ particles. Therefore,

a sharp increase in the viscosities of the $Nd_2O_3/SiO_2$-STF is observed.

## 5. Conclusions

In this study, the $Nd_2O_3/SiO_2$-STF samples were prepared with different mass ratio values and tested. The microscopic characterization and the steady rheological properties of $Nd_2O_3/SiO_2$-STF were investigated. The effect of temperature on its dynamic rheological properties was specifically studied.

The results demonstrate that the addition of $Nd_2O_3$ particle significantly influenced the rheological properties of $SiO_2$-STF. $Nd_2O_3/SiO_2$-STF showed significant shear thinning and ST behaviour. When the mass fraction of $Nd_2O_3$ particle was 12%, the rise in the peak viscosity of $Nd_2O_3/SiO_2$STF was the largest. Compared to $SiO_2$-STF, $12\%Nd_2O_3/20\%SiO_2$-STF not only increased the peak viscosity by 3.21 times, but also reduced the critical rate of the system by 74.86%. Importantly, the initial viscosity of the system was only 219.29 Pa.s, which was close to the ST peak viscosity of the suspension. Therefore, $12\%Nd_2O_3/20\%SiO_2$-STF is observed to be more suitable for impregnated fabric to improve the ballistic impact.

In addition, the ST effect of $Nd_2O_3/SiO_2$-STF was highly significant with the increase in the $Nd_2O_3$ particle mass fraction at lower temperatures, while the shear thinning behaviour weakened. More importantly, at higher temperatures, the ST properties were remarkable, and became highly remarkable with the increase in the $Nd_2O_3$ particle mass fraction. Moreover, when the temperature was high at 50°C and the mass fraction of $Nd_2O_3$ particle was 12%, the corresponding ST effect was 13.49, which is 5.18 times that of the single $SiO_2$-STF. As a result, $12\%Nd_2O_3/20\%SiO_2$-STF is suggested to be suitable for use in vibration control devices, which require a high temperature environment.

## Acknowledgements

We acknowledge financial support from the National Key R&D Program of China (Grant No. 2018YFC1504303). We are extremely grateful to the anonymous reviewers for their valuable criticisms and useful suggestions that aided in improving the quality of this work.

## References

[1] Tian T and Nakano M 2017 *Smart Mater. Struct.* **26** 035038
[2] Qin J, Zhang G and Shi X 2016 *J. Dispersion Sci. Technol.* **37** 1599
[3] Wu X-J, Wang Y, Yang W, Xie B-H, Yang M-B and Dan W 2012 *Soft Matter* **8** 10457
[4] Nakonieczna P, Wierzbicki Ł, Wróblewski R, Płociński T and Leonowicz M 2019 *Bull. Mater. Sci.* **42** 162
[5] Lee B-W and Kim C-G 2012 *Adv. Compos. Mater.* **21** 177
[6] Hasanzadeh M and Mottaghitalab V 2014 *J. Mater. Eng. Perform.* **23** 1182
[7] Gurgen S and Kushan M C 2017 *Polym. Test.* **64** 296
[8] Pinto F and Meo M 2017 *Appl. Compos. Mater.* **24** 643
[9] Yeh F-Y, Chang K-C, Chen T-W and Yu C-H 2014 *J. Chin. Inst. Eng.* **37** 983
[10] Lin K, Liu H, Wei M, Zhou A and Bu F 2018 *Smart Mater. Struct.* **28** 025007
[11] Wei M, Hu G, Li L and Liu H 2018 *Meccanica* **53** 1
[12] Ge J H, Tan Z H, Li W H and Zhang H 2017 *Results Phys.* **7** 3369
[13] Gürgen S, Kuşhan M C and Li W 2016 *Korea-Aust. Rheol. J.* **28** 121
[14] Sha X, Yu K, Cao H and Qian K 2013 *J. Nanopart. Res.* **15** 1816
[15] Ghosh A, Chauhan I, Majumdar A and Butola B S 2017 *Cellulose* **24** 4163
[16] Jiang W, Sun Y, Xu Y, Peng C, Gong X and Zhang Z 2010 *Rheol. Acta* **49** 1157
[17] Xu Y-L, Gong X-L, Peng C, Sun Y-Q, Jiang W-Q and Zhang Z 2010 *Chin. J. Chem. Phys.* **23** 342
[18] Qin J, Zhang G, Shi X and Tao M 2015 *J. Nanopart. Res.* **17** 333
[19] Tian T, Peng G, Li W, Ding J and Nakano M 2015 *Korea-Aust. Rheol. J.* **27** 17
[20] Yue C-F, Huang S-J, Chen J-K, Li H-T and Chan K-S 2018 *Met. Mater. Int.* **24** 307
[21] Gu M Y, Wei G L, Liu W C and Wu G H 2017 *Mater. Corros.* **68** 436
[22] Wang S-N, Sun M-M, Huang M-L, Cheng T-Q, Wang J-L, Yuan S-D *et al* 2017 *Mol. Catal.* **433** 162
[23] He Q, Gong X, Xuan S, Jiang W and Chen Q 2015 *J. Mater. Sci.* **50** 6041
[24] Hasanzadeh M, Mottaghitalab V, Babaei H and Rezaei M 2016 *Compos. Part A: Appl. Sci. Manuf.* **88** 263
[25] Wei M, Sun L, Zhang C, Qi P and Zhu J 2019 *J. Mater. Sci.* **54** 346
[26] Liu X-Q, Bao R-Y, Wu X-J, Yang W, Xie B-H and Yang M-B 2015 *RSC Adv.* **5** 18367